Available online at www.sciencedirect.com
ScienceDirect
ELSEVIER
Geomorphology xx (2007) xxx–xxx
GEOMORPHOLOGY
www.elsevier.com/locate/geomorph

Internal characteristics of ice-marginal sediments deduced from georadar profiling and sediment properties (Brøgger Peninsula, Svalbard)

Georg Schwamborn [a,*], Johannes Heinzel [b], Lutz Schirrmeister [a]

[a] *Alfred Wegener Institute for Polar and Marine Research, Telegrafenberg A43, D-14473 Potsdam, Germany*
[b] *Geographisches Institut Johannes Gutenberg Universität, D-55099 Mainz, Germany*

Received 12 May 2005; received in revised form 1 December 2005; accepted 10 July 2006

Abstract

Georadar and sedimentological data were acquired in the Ny-Ålesund area on Brøgger Peninsula in order to study diamicton in frontal areas of Vestre Brøggerbreen and Midre Lovénbreen. Parallel common offset georadar lines were acquired for information on thickness and layering and multioffset measurements served to deduce the subground velocity. Short permafrost cores (<3 m depth) were extracted for ground verification. Several stratigraphic properties from the cored frozen sediments (i.e. grain size, ice content, total carbon content) allow characterizing the glacial detritus and sediment changes exciting electromagnetic reflections. Site dependent georadar data suggest that prominent reflections mainly coincide with sediment changes such as in ice content or major lithotype change. For example, at one site the contact to the underlying bedrock could be made visible and the moraine thickness could be inferred. In case of a discrete ice layer georadar trace modelling has helped to support interpretation of field measurements. Results of this study suggest that carbonaceous and clay-rich diamicton attenuates the electromagnetic wave propagation more than carbon-poor and clay-poor sediments.

Keywords: Ground-penetrating radar; Svalbard; Glacial sediments; Permafrost

1. Introduction

Georadar or ground-penetrating radar (GPR) is a long established tool in structural surveys of frozen ground (Annan and Davis, 1976; Arcone et al., 1998; Arcone et al., 2002). In polar areas GPR wave reflections can be generated due to differences in the ground ice content, from interfaces between water tables, bedrock, the active layer, and permafrost (Arcone et al., 1998; Arcone and Delaney, 2003). Within frozen sediments effects of geocryologic phenomena and their stratigraphic properties (e.g. ice bands and ice lenses) can cause georadar reflections (Annan and Davis, 1976; Moorman et al., 2003). On Svalbard the past years have seen a focus on studying the transition of glacial to periglacial areas, where there has been made use of georadar profiles particularly for structural studies of debris-rich proglacial areas of valley glaciers (Hambrey et al., 2005). Thrust features within surging glacier mouths (Murray et al., 1997) and (sub-)basal sediment-rich glacier ice were delineated using georadar signals (Murray et al., 2000; Smith et al., 2002). Survey

* Corresponding author. Tel./fax: +49 331 288 2162/37.
E-mail address: gschwamborn@awi-potsdam.de (G. Schwamborn).

0169-555X/$ - see front matter © 2007 Elsevier B.V. All rights reserved.
doi:10.1016/j.geomorph.2006.07.032

continuity into the morainic environment in front of the glaciers has been made in a detailed sedimentologic manner (Hambrey et al., 1997, 1999; Glasser et al., 1999). However, using georadar in frozen proglacial deposits for reconnaissance and palaeo environmental reconstruction seems to be exceptional (Lønne and Lauritsen, 1996). Instead, in periglacial environments with permafrost conditions it was more applied to internal structures of rock glaciers (Berthling et al., 2000; Isaksen et al., 2000).

The objective of this study is to show and assess benefits and limits of georadar in proglacial terrain. In particular, this technique helps to differentiate the internal structure of poorly sorted frozen sediments (permafrost). Perspectively, subsurface information should be combined with surface mapping, and contribute to understanding the development of Late Quaternary landforms in glacial and periglacial environments.

1.1. Study area

Two different sites on Brøgger Peninsula, W-Spitsbergen, were selected (Fig. 1), both of which are situated in continuous permafrost in front of the glacier margins with a reported permafrost depth of up to 140 m (Liestøl, 1980).

Location 1 is at Knudsenheia, a near-coastal and ice-free area in front of Vestre Brøggerbreen about 3 km NW of Ny-Ålesund (Fig. 1). It belongs to a series of post-glacially emerged beach lines. The Late Weichselian glacier retreat and the post-glacial uplift as documented in raised marine terraces in the area have intensively been studied (e.g. Forman et al., 1987; Landvik et al., 1987; Héquette, 1987; Lehman and Forman, 1992; Andersson et al., 2000). Accordingly, the terrace of location 1 is mapped as a marine deposit (Kristiansen and Sollid, 1987) and considered as a glaciomarine moraine created by an ice shelf glacier. At present, the surface has vegetation cover and mainly snowmelt affects the drainage (Laffly and Mercier, 2002). The grid of georadar lines is placed upon a measuring field, which is part of the global CALM *(Circumpolar Active Layer Monitoring)* initiative. Ongoing monitoring of active layer thickness shows maximum values of 75 to 80 cm (Christiansen, 2007).

Location 2 is situated in the forefield of Midre Lovénbreen, about 3 km SE of Ny-Ålesund (Fig. 1). The ice-proximal paraglacial area is affected by sheet wash and rill wash during spring and summer season and holds predominantly pebbly to silty-sandy deposits that fill a fan-like system of gullies. It is fed by the melt-out of the glacier and is constantly modified by water action during summer seasons (Laffly and Mercier, 2002). Outwash plains are

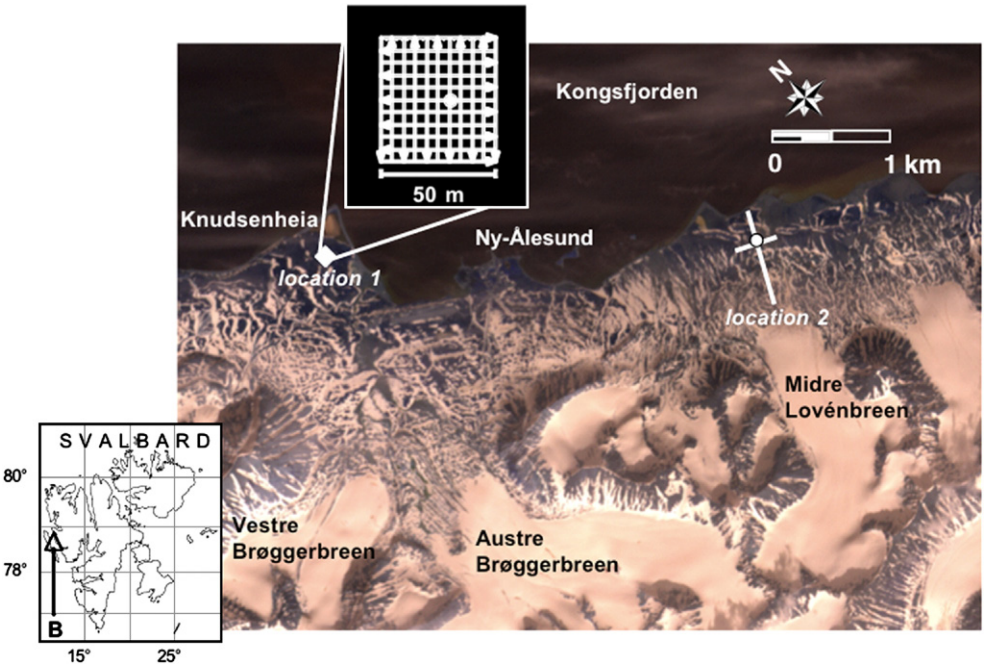

Fig. 1. A satellite image of the Ny-Ålesund area on Brøgger Peninsula (bold B, lower inset), Spitsbergen, Svalbard archipelago. It shows the study sites at Knudsenheia (location 1) and the glacier forefield of Midre Lovénbreen (location 2) with associated sketches of the georadar survey lines. Dots mark coring places.

Please cite this article as: Schwamborn, G. et al. Internal characteristics of ice-marginal sediments deduced from georadar profiling and sediment properties (Brøgger Peninsula, Svalbard). Geomorphology (2007), doi:10.1016/j.geomorph.2006.07.032

rather typical landscape features along the northeast coast of the Brøgger Peninsula, where several glacier tongues terminate in a short distance to Kongsfjorden. Their end moraines mark the neoglacial maximum (late nineteenth/early twentieth centuries) (Glasser and Hambrey, 2001). Outcropping rocks in the glacier forefield consist of Paleozoic formations including dolomite breccias and marl (Hjelle et al., 1999).

2. Methods

2.1. Georadar data characteristics

Georadar transmits electromagnetic pulses into the ground and receives echoes from reflecting subsurface boundaries, across which there are contrasts in the relative dielectric permittivity. The relative permittivity (ε_r) describes the potential to polarize materials. It is high in water ($\varepsilon_{r(water)}=87$ at 0 °C) and particularly low in frozen material ($\varepsilon_{r(ice)}=3$–4; Davis and Annan, 1989; $\varepsilon_{r(permafrost)}=4$–8; Daniels, 1996). This makes it attractive for frozen ground studies, since liquid water rapidly attenuates electromagnetic wave propagation. However, the frozen state of sediments can also decrease the detectability of physical contrasts, which otherwise would be pronounced through differing water contents. Also, mineralogy influences detectable contrasts with loamy dry soil ($\varepsilon_r=4$–6; Daniels, 1996), dry limestone ($\varepsilon_r=7$; Daniels, 1996) and clay ($\varepsilon_r=5$–40; Davis and Annan, 1989) having different permittivities. Energy that is not reflected continues to the next interface or until it is attenuated with depth. The propagation velocity of electromagnetic waves in geological media can be expressed by

$$v = c_o/\sqrt{\varepsilon_r} \quad (1)$$

where v is the velocity and c_o is the electromagnetic wave velocity in a vacuum (0.3 m/ns). For permafrost the velocity is commonly above that of wet but unsaturated sediments (0.06 m/ns) and below that of pure ice (0.17 m/ns). Propagation velocity is critical for estimating the vertical resolution. Approximated from the selected antenna frequency the optimum vertical resolution can be a quarter of a wavelength (Sheriff and Geldart, 1995), whereby the wavelength (λ) depends on the velocity in the relevant material and the dominant frequency (f) such that:

$$\lambda = v/f \quad (2)$$

An approximate vertical resolution for a 100 MHz signal in permafrost is about 0.4 m (Schwamborn et al., 2002). Complementary, results of sediment coring were taken to calibrate the propagation velocity between two distinct reflectors that could be verified by sediment change.

2.2. Data acquisition

The used georadar equipment consisted of a 100 MHz antenna pair (commercial RAMAC/GPR acquisition system) that was a reasonable trade-off between penetration and resolution characteristics and mobility in the field. The transmitter–receiver distance had a constant offset of 1 m and trace spacing was 0.5 m during profiling in a 750 ns time window containing 1024 samples. The instrument was pulled manually and data have been measured parallel to the profile direction. 2-D georadar lines were orientated parallel and orthogonal allowing for intersecting profiling. Measurements were performed during spring season 2002 when there was a snow cover of about 30 cm. Standard processing enhanced the reflection profiles including a time-zero adjustment, a removal of low frequency noise, topographic correction, migration, wherever necessary, and an automatic gain function. In addition, two shallow cores, one for each site and about 3 m in length, were extracted for complementary stratigraphic studies. Prior to sediment coring multioffset common-midpoint (CMP) recordings were collected above the coring site to obtain velocity measurements. CMP soundings can be used to infer both the depth of reflecting interfaces and the propagation velocity (Annan and Davis, 1976). Starting with a minimal offset of 1 m traces were recorded at 0.25 m or 0.5 m offset increments with a 32-fold stack applied to each trace.

2.3. Sediment sampling

For permafrost recovery a rotary-coring device (TKB 15, L. Kurth Corp.) was taken, which was powered by a 2 HP engine and had a core diameter of 6 cm. Cryotexture, sediment type, and colour were recorded in the field and samples were kept in frozen state and tightly wrapped in plastic liners for transit to the laboratory. Subsampling in the laboratory was done in 5 cm intervals or at visible sediment boundaries. The samples were measured for gravimetric ice content (expressed as water equivalent), for grain sizes composition, and for total carbon content in order to identify lithologic differences possibly influencing wave propagation. Water content was determined after freeze-drying and taking the difference between the original and the dried sample. Grain sizes were measured using a

Please cite this article as: Schwamborn, G. et al. Internal characteristics of ice-marginal sediments deduced from georadar profiling and sediment properties (Brøgger Peninsula, Svalbard). Geomorphology (2007), doi:10.1016/j.geomorph.2006.07.032

laser particle sizer (LS200, Beckmann-Coulter Corp.) for the clay–silt–sand fractions and a sieve for the pebble fraction to determine fraction percentages. The total carbon content (TC) was measured in a chemical elemental analyser (VARIO EL III) and is expressed in weight percent (wt.%). The TC value overall reflects carbon content of inorganic origin since no visible organic remains could be detected and test measurements yielded a negligible organic content (<5% of 100% TC). The TC value is, thus, considered to represent carbonate content.

3. Results and discussion

In the following representative profiles are discussed that contain the main reflection features. During profiling the snow cover was 0.3 m thick, which in terms of GPR characteristics is principally below the pulse resolution given a reasonable velocity of 0.23 m/ns for snow ($\varepsilon_r = 1.7$). This velocity has been deduced from surface waves measured at another site not shown here.

At location 1 (Knudsenheia) a set of 50 m long profiles is displayed that all show similar signal penetration to about 50 ns time delay (Fig. 2). This short delay indicates either a considerable energy loss factor in the material or ground without distinct sediment layers at greater depths. After the first arrivals of the direct air and ground waves, the first reflections (b1–b5) exhibit some moderately continuous reflectors in the subground. Some of the reflectors appear to be single-line events, whereas others occur within two or three consecutive lines. They are interpreted to represent various sediment layers. From line b5 to line b11 there is a distinct reflector visible at about 50 ns travel time with some lateral continuity in each profile even though amplitude strength is variable (see arrows). It is strongest in lines b5 and b6 and weaker in the subsequent lines. However, here a lateral continuity is more pronounced with an increasing upward bending to the eastern end of the profile (lines b9 to b11). To identify this reflection event velocity and borehole studies were carried out in the middle part of line b5, where the amplitude strength is strongest. The relevant

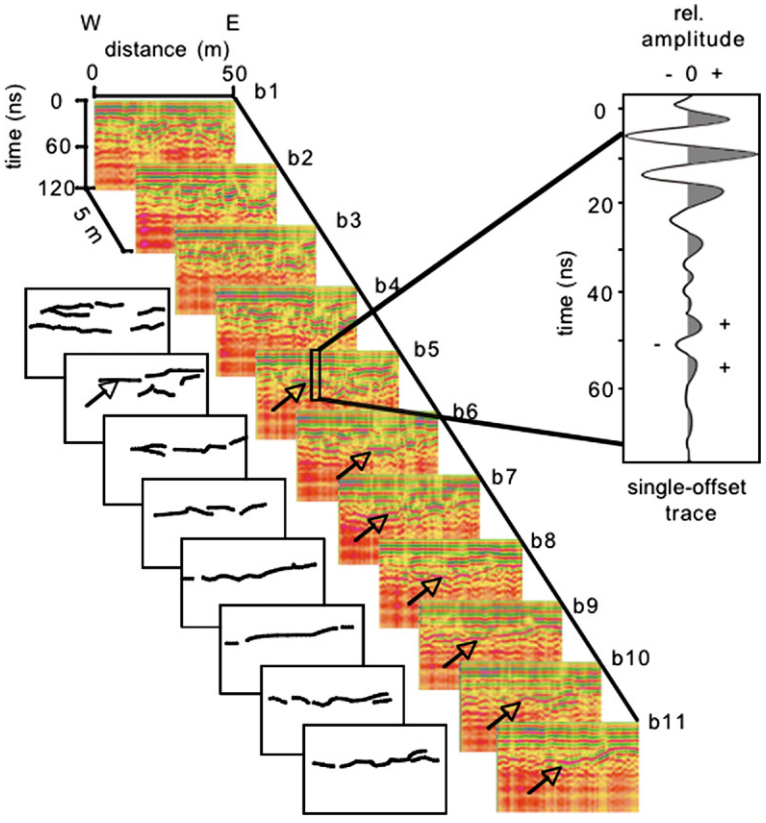

Fig. 2. 100 MHz survey in a 50 m field at location 1. The arrows point to a subground reflector, which can be followed over several lines. In the sketches to the left straight lines highlight prominent reflectors and pointed lines to other reflection events. Enlarged to the right is an example trace hitting a prominent single reflector that was subject to further studies. Signal processing included bandpass filtering and migration.

Please cite this article as: Schwamborn, G. et al. Internal characteristics of ice-marginal sediments deduced from georadar profiling and sediment properties (Brøgger Peninsula, Svalbard). Geomorphology (2007), doi:10.1016/j.geomorph.2006.07.032

wavelet shows a double positive response at the reflection interface (between 45 and 55 ns) (Fig. 2).

The multioffset profile confirms the event delineated from the parallel lines (Fig. 3). At first the air wave is recorded with a slope pointing to the velocity speed in air of vacuum (0.3 m/ns). For an unknown reason the slope of the ground roll is missing. The reflector at 45 ns two-way travel time reveals a hyperbolic slope documenting an interval velocity of 0.125 m/ns. This accounts for $\varepsilon_r = 5.7$ for the frozen subground following formula (1) and an estimated target depth of 2.8 m.

A short permafrost core (2.95 m sediment recovery) was extracted at this site for ground verification. The sediment profile is principally made up of morainic deposits with the following material properties from the bottom to the top. The lowermost part of the core (2.95 to 2.55 m sediment depth) consists of massive ice that has some silty streaks in it. The ice content in this layer reaches partly beyond 40 wt.%. A 20 cm thick pebble-rich layer with a silty matrix and low ice content that decreases to less than 10 wt.% overlies it. The subsequent core part (2.35 to 0.0 m sediment depth) consists of a diamictic substrate that has no peculiar macroscopical layering. Substrate variations here are best expressed in grain size changes, especially in the course of the pebble-sized fraction (Fig. 4). TC values show that the bottom core part (2.95 m to 0.85 m sediment depth) is characterized by relatively high TC values (up to 8 wt.%), whereas the upper part (0.85 to 0 m sediment depth) has low TC values (<4 wt.%). The boundary at 0.85 m is regarded as the lowermost depth, to which carbonate has been dissolved in the active layer and washed out downhill during previous summer seasons. The depth agrees fairly well with the active layer depths measured in the CALM programme conducted at this site (Humlum, 2005).

Using the core logging to calibrate the georadar reflection depths the frozen moraine shows a value of $\varepsilon_r = 5.6$, and a velocity of 0.127 m/ns, respectively. This harmonizes with the value deduced from the CMP record. To confirm the interpretation that the recovered ice layer has caused the pronounced georadar reflection, a finite difference (FD) waveform modelling was calculated with the core stratigraphy and the measured and estimated permittivity values as input parameters. From top to the bottom the values are listed in Table 1. For completeness the snow layer has been added to the model. The ice layer is expressed by a commonly measured value of $\varepsilon_r = 2.8$ (Eisen et al., 2002). The trace comparison shows a fairly good matching of the +–+ amplitude event at 50 ns in both the field and the synthetic wavelet at the relevant depth (Fig. 5). A slight

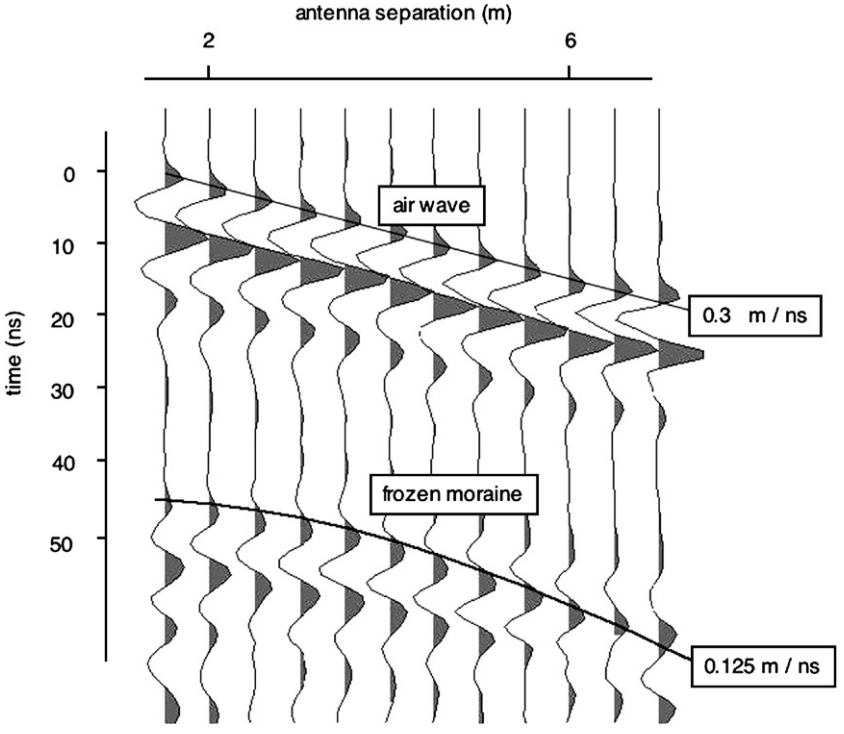

Fig. 3. The multioffset (CMP) record at location 1 reveals a frozen ground velocity of 0.125 m/ns.

Please cite this article as: Schwamborn, G. et al. Internal characteristics of ice-marginal sediments deduced from georadar profiling and sediment properties (Brøgger Peninsula, Svalbard). Geomorphology (2007), doi:10.1016/j.geomorph.2006.07.032

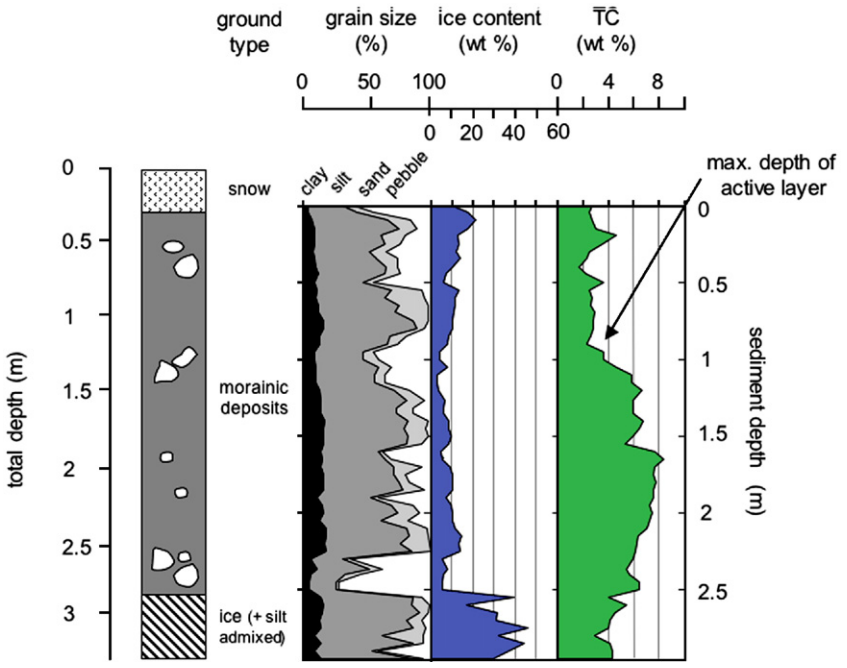

Fig. 4. Cryo- and sedimentological layers of a short permafrost core sampled within the georadar field of location 1 (GPS coordinates: N 78°56′18″, E 11°50′40″). The arrow indicates the maximum summerly active layer depth. Note the ice-poor pebbly layer between 2.35 and 2.55 m sediment depth.

difference is seen when comparing the modelled diamicton thickness of 2.4 m (see Table 1) with the cored thickness of 2.55 m (Fig. 4) to produce this similar reflection event at the same depth position. However, the difference lies within the vertical resolution error. Thus, a single ice layer in the model mimics a realistic assumption that the cored ice layer is associated with the reflection event.

At location 2 a profile crossing from SW to NE the glaciofluvial forefield of Midre Lovénbreen (Fig. 6) has a distinct and fairly continuous reflector separating an upper from a lower unit. The interface runs from NE to SW in 5 to 20 m sediment depths at maximum (Fig. 7). It is interpreted as the contact between the upper glacial sediment fill (morainic deposits) and the underlying Paleozoic rocks. The aerial photograph (Fig. 6), where Paleozoic outcrops frame the proglacial plain, and the subsurface boundary of the morainic deposits illustrate that a basinal depression in front of the glacier tongue has been excavated and subsequently filled with glacial detritus. An intersecting profile zooms into the contact area of both rock types (Fig. 7). As endpoints of this intersecting profile Paleozoic outcrops have been used.

Table 1
Input parameters used for trace modelling as deduced from core results

Material	Wavelength (m)	Wave velocity (m/ns)	ε_r	Thickness (m)
Snow	2.3	0.23	1.7	0.3
Permafrost	1.27	0.127	5.6	2.4
Ice	1.8	0.18	2.8	0.4

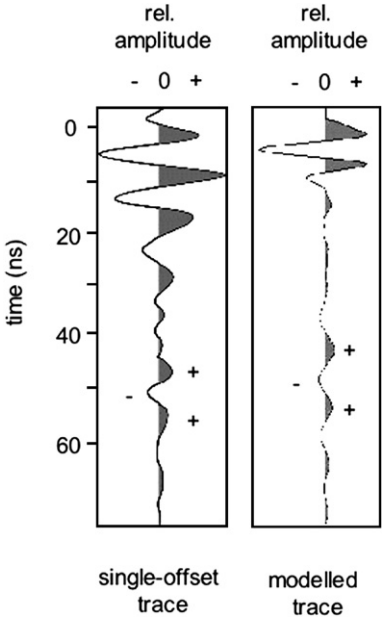

Fig. 5. Field trace and modelled trace with similar +–+ reflector events. Input parameters are taken from core results at location 1 (see Table 1).

Please cite this article as: Schwamborn, G. et al. Internal characteristics of ice-marginal sediments deduced from georadar profiling and sediment properties (Brøgger Peninsula, Svalbard). Geomorphology (2007), doi:10.1016/j.geomorph.2006.07.032

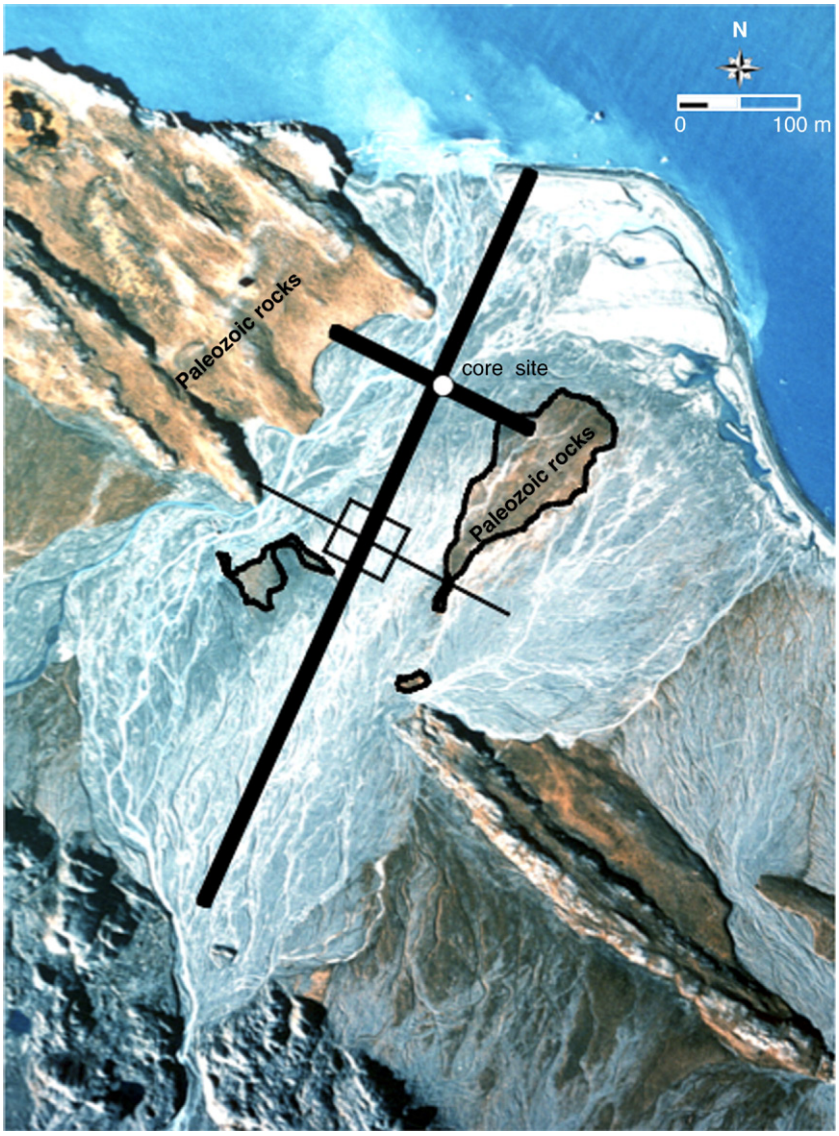

Fig. 6. 100 MHz survey field at location 2. Bold lines mark profiles discussed in the text. The complementary coring site is added (white dot). Note the outcropping Paleozoic rocks (dashed lines). Aerial photograph S95 1096, published with permission from Norsk Polarinstitutt.

It appears that the contact between the upper frozen glacigenic sediments and the Paleozoic bed rocks that are also subject to permafrost conditions is not strong enough at all places to electromagnetically expose the lithologic change. This is valid especially for the NW end of the profile.

A complementary short permafrost core (3.1 m sediment recovery) taken in the middle part of the profile shows a diamictic composition typical for glacigenic sediments (Fig. 8). The layers of snow and ice on top of frozen sediments are not resolved in the respective radargrams and masked by air and ground waves.

From the core bottom upwards the sediment facies consists of a poorly sorted, morainic facies with a high portion of pebble-sized clasts (3.1 to 0.7 m sediment depth). This core part is followed to the top by a 70 cm thick silt to sand dominated, partly pebble-rich facies. The transition into the pebble-rich facies is interpreted as marking outwash deposits in higher energy channel environment. It is remarkable that the TC values in the sediments are clearly lower (0.5% in average) compared to the measurements from location 1 (5% in average). Also, the clay content at location 2 is on average smaller (9.2%) than at location 1 (12.4%). As introduced earlier both lithologic properties are associated with potentially

Please cite this article as: Schwamborn, G. et al. Internal characteristics of ice-marginal sediments deduced from georadar profiling and sediment properties (Brøgger Peninsula, Svalbard). Geomorphology (2007), doi:10.1016/j.geomorph.2006.07.032

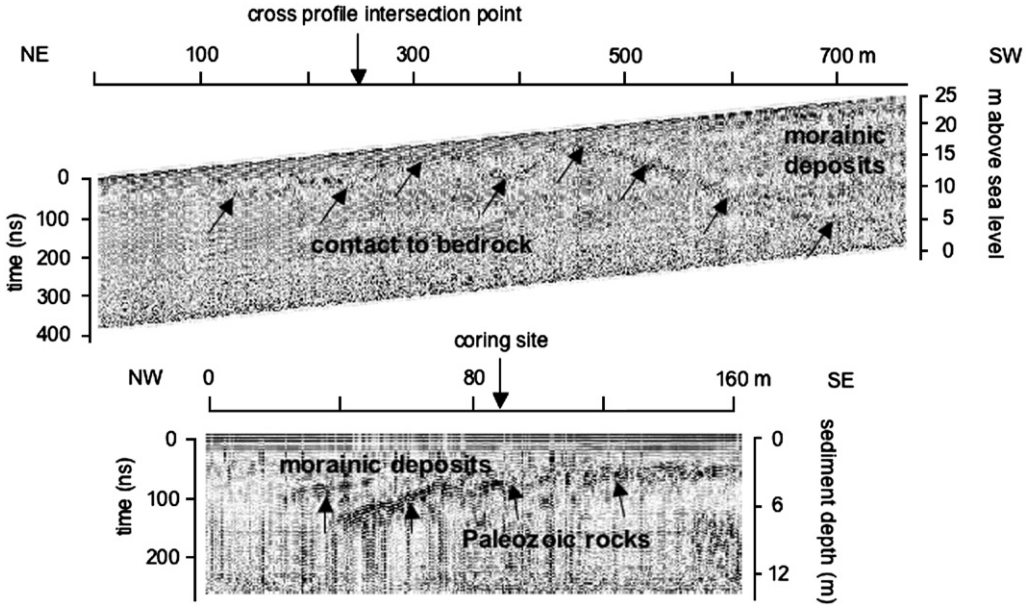

Fig. 7. Two 100 MHz profiles at location 2. Scale bar assumes the same subground velocity as for location 1.

higher permittivities. This is taken as an indication that a carbonate-poor sedimentary environment like location 2 allows for better electromagnetic penetration, since calcite ($CaCO_3$), a major constituent of the matrix, has a permittivity of 8 to 9, nearly twice the permittivity of quartz (ε_r=4.6) (Lebron et al., 2004). However, let us not forget that there is an uncertainty of radar wave scattering in poorly sorted sediments containing a considerable portion of pebble-sized clasts as it is present at both sides. Secondly, latent water occurrence in pore spaces around sediment grains, especially in clayey parts, even at temperatures down to −12 °C

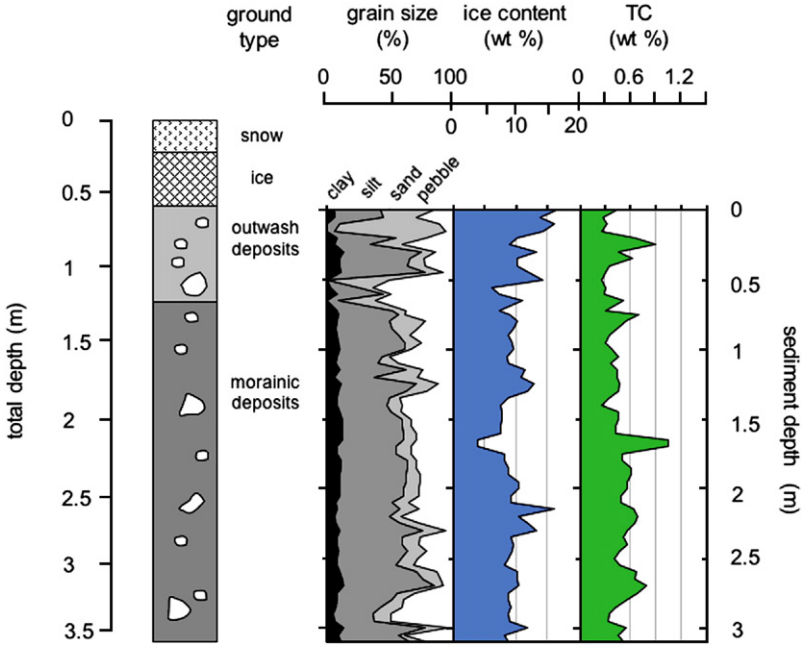

Fig. 8. Cryo- and sedimentological layers of a short permafrost core sampled within the georadar field of location 2 (GPS coordinates: N 78°54′32″, E 12°06′05″).

Please cite this article as: Schwamborn, G. et al. Internal characteristics of ice-marginal sediments deduced from georadar profiling and sediment properties (Brøgger Peninsula, Svalbard). Geomorphology (2007), doi:10.1016/j.geomorph.2006.07.032

(Boike et al., 1998) cannot be excluded and could account for further wave attenuation by increasing permittivity values. Geomorphic surface mapping with focus on glacigenic sediments and log profiling from various locations in the Midre Lovenbreen proglacial terrain shows a generally 1–2 m thick "clast-rich muddy diamicton (basal till)" on top of "muddy sandy gravel" of unknown thickness (Glasser and Hambrey, 2001). This sedimentary interface is not well expressed in the GPR records, which also suggests that coarse-grained but poorly sorted ground in this case has hampered resolution of the facies boundary. Higher frequency antennas could allow for better resolution of this near-surface horizontal boundary (e.g. 200 MHz radargrams in Lønne and Lauritsen, 1996). In concert with more ground verification this may improve correlation of sedimentologic and georadar observations.

4. Conclusions

A combination of common offset and multioffset georadar measurements, sediment properties and wavelet modelling was successfully used to extract subground details from low to moderate penetration, pebble-rich diamictic frozen sediments. At location 1 a discrete target like a single ice layer could be detected within a frozen sediment package. It is expressed as a difference of greater than 30 wt.% in ice content, shows a spatial extension of at least several tens of metres, and is mirrored in wavelet modelling.

Site-dependent results suggest that electromagnetic wave penetration is associated with overall carbonate and clay content. Namely at location 2 maximum penetration was gained in a carbonate-poor and clay-poor diamicton where a basinal moraine geometry and thickness of up to 20 m are inferred. However, results of sedimentary log profiling are not straightly mirrored in the GPR lines. Usage of higher frequency antennae for improving resolution characteristics in the near-surface subground (<3 m depth) is recommended for future studies.

Acknowledgments

Our gratitude is addressed to H.-W. Hubberten and R. Neuber from AWI-Potsdam, to C. Wille, M. Wolff and Y. Kramer at Koldewey-Station (project no.: KOP 78), and to O. Humlum and J. Kohler; all of them supported this study at various stages. G. Rachlewicz and anonymous provided valuable comments on an earlier version of the manuscript. They helped to improve this paper.

References

Annan, A.P., Davis, J.L., 1976. Impulse radar sounding in permafrost. Radio Science 11, 383–394.

Arcone, S.A., Delaney, A.J., 2003. Radiowave pulse refraction and ground wave propagation through permafrost and the active layer. In: Phillips, Springman, Arendson (Eds.), Int. Permafrost Conference. Swets & Zeitlinger, Lisse. ISBN: 90 5809 5827, pp. 21–25.

Arcone, S.A., Lawson, D.E., Delaney, A.J., Strasser, J.C., Strasser, J.D., 1998. Ground-penetrating radar reflection of groundwater and bedrock in an area of discontinuous permafrost. Geophysics 63 (5), 1573–1584.

Arcone, S.A., Prentice, M.L., Delaney, A.J., 2002. Stratigraphic profiling with ground penetrating in permafrost: a review of possible analogs for Mars. Journal of Geophysics 107 (E11), 5108. doi:10.1029/2002JE001906.

Andersson, T., Forman, S.L., Ingólfsson, Ó., Manley, W.F., 2000. Stratigraphic and morphologic constraints on the Weichselian glacial history of northern Prins Karls Forland, western Svalbard. Geografiska Annaler 82 A, 455–470.

Berthling, I., Etzelmüller, B., Isaksen, K., Sollid, J.L., 2000. Rock glaciers on Prins Karls Forland. II: GPR soundings and the development of internal structures. Permafrost and Periglacial Processes 11, 357–369.

Boike, J., Roth, K., Overduin, P.P., 1998. Thermal and hydrologic dynamics of the active layer at a continuous permafrost site (Taymyr Peninsula, Siberia). Water Resources Research 34/3, 355–363.

Daniels, D.J., 1996. Surface penetrating radar. IEE Radar, Sonar, Navigation and Avionics Series, vol. 6. The Institute of Electrical Engineers, London. 320 pp.

Davis, J.L., Annan, A.P., 1989. Ground-penetrating radar for high resolution mapping of soil and rock stratigraphy. Geophysical Prospecting 37, 531–551.

Eisen, O., Nixdorf, U., Wilhelms, F., Miller, H., 2002. Electromagnetic wave speed in polar ice: validation of the CMP technique with high-resolution dielectric profilling and g-density measurements. Annals of Glaciology 34, 150–156.

Forman, S.L., Mann, D.H., Miller, G.H., 1987. Late Weichselian and Holocene relative sea-level history of Brøggerhalvøya, Spitsbergen. Quaternary Research 27, 41–50.

Glasser, N.F., Hambrey, M.J., 2001. Styles of sedimentation beneath Svalbard valley glaciers under changing dynamic and thermal regimes. Journal of the Geological Society 158 (4), 697–707 (11).

Glasser, N.F., Hambrey, M.J., Bennett, M.R., Huddart, D., 1999. The morphology, composition and origin of medial moraines on polythermal glaciers in Svalbard. Glacial Geology and Geomorphology http://boris.qub.ac.uk/ggg/papers/full/1999/rp071999/rp07.html.

Hambrey, M.J., Huddart, D., Bennett, M.R., Glasser, N.F., 1997. Genesis of 'hummocky moraines' by thrusting in glacier ice: evidence from Svalbard and Britain. Journal of the Geological Society, London 154, 623–632.

Hambrey, M.J., Glasser, N.F., Crawford, K., Bennett, M.R., Huddart, D., 1999. Facies and landforms associated with ice deformation in a tidewater glacier, Svalbard. Glacial Geology and Geomorphology http://boris.qub.ac.uk/ggg/papers/full/1999/rp071999/rp07.html.

Hambrey, M.J., Murray, T., Glasser, N.F., Hubbard, A., Hubbard, B., Stuart, G., Hansen, S., Kohler, J., 2005. Structure and changing dynamics of a polythermal valley glacier on a centennial timescale: Midre Lovenbreen, Svalbard. Journal of Geophysical Research 110, F01006. doi:10.1029/2004JF000128.

Héquette, A., 1987. Holocene vertical shoreline displacement in northwest Spitzbergen, Svalbard: new interpretation. The example of Brøggerhalvøya. Norsk Geografisk Tidsskrift 41, 91–100.

Please cite this article as: Schwamborn, G. et al. Internal characteristics of ice-marginal sediments deduced from georadar profiling and sediment properties (Brøgger Peninsula, Svalbard). Geomorphology (2007), doi:10.1016/j.geomorph.2006.07.032

Hjelle, A., Piepjohn, K., Saalmann, K., Salvigsen, O., Thiedig, F., Dallmann, K., 1999. Geological map Svalbard 1:100 000 Spitsbergen, sheet A7G Kongsfjorden, Norsk Polarinstitutt, Tromsø, 56 pp.

Christiansen, H., 2007. Monitoring active layer thickness and temperatures, a CALM-project http://www.unis.no/RESEARCH/GEOLOGY/Geo_research/Hanne/CALM.htm.

Isaksen, K., Ødegard, R.S., Eiken, T., Sollid, J.L., 2000. Composition, flow and development of two tongue-shaped rock glaciers in the permafrost of Svalbard. Permafrost and Periglacial Processes 11, 241–257.

Kristiansen, K.J., Sollid, J.L., 1987. Svalbard Jordartskart (Map of Surficial Materials), Nasjonalatlas for Norge, Kartblad 2.3.6. Geografisk Institutt Universitetet i Oslo.

Laffly, D., Mercier, D., 2002. Global change and paraglacial morphodynamic modification in Svalbard. International Journal of Remote Sensing 23 (21), 4743–4760.

Landvik, J.Y., Mangerud, J., Salvigsen, O., 1987. The Late Weichselian and Holocene shoreline displacement on the west-central coast of Svalbard. Polar Research 5, 29–44.

Lebron, I., Robinson, D.A., Goldberg, S., Lescha, S.M., 2004. The dielectric permittivity of calcite and arid zone soils with carbonate minerals. Soil Science Society of America Journal 68, 1549–1559.

Lehman, S.J, Forman, S.L., 1992. Late Weichselian glacier retreat in Kongsfjorden, West Spitsbergen, Svalbard. Quaternary Research 37, 139–154.

Liestøl, O., 1980. Permafrost conditions in Spitsbergen. Frost i Jord 23–28.

Lønne, I., Lauritsen, T., 1996. The architecture of a modern push-moraine at Svalbard, as inferred from ground-penetrating radar measurements. Arctic and Alpine Research 28, 488–495.

Moorman, B.J., Robinson, S.D., Burgess, M.M., 2003. Imaging periglacial conditions with ground-penetrating radar. Permafrost and Periglacial Processes 14, 319–329.

Murray, T., Gooch, D.L., Stuart, G.W., 1997. Structures within the surge front at Bakaninbreen, Svalbard, using ground-penetrating radar. Annals of Glaciology 24, 122–129.

Murray, T., Stuart, G.W., Miller, P.J., Woodward, J., Smith, A.M., Porter, P.R., Jiskoot, H., 2000. Glacier surge propagation by thermal evolution at the bed. Journal of Geophysical Research 105 (B6), 13491–13507.

Schwamborn, G., Dix, J.K., Bull, J.M., Rachold, V., 2002. Ground penetrating radar and high-resolution seismics—geophysical profiling of a thermokarst lake in the western Lena Delta, N-Siberia. Permafrost and Periglacial Processes 13 (4), 259–269.

Sheriff, R.E., Geldart, L.P., 1995. Exploration Seismology. Cambridge. 592 pp.

Smith, A.M., Murray, T., Davison, B.M., Clough, A.F., Woodward, J., Jiskoot, H., 2002. Glacier surge propagation by thermal evolution at the bed. Journal of Geophysical Research 107 (B8). doi:10.1029/2001JB000475.

Please cite this article as: Schwamborn, G. et al. Internal characteristics of ice-marginal sediments deduced from georadar profiling and sediment properties (Brøgger Peninsula, Svalbard). Geomorphology (2007), doi:10.1016/j.geomorph.2006.07.032